ELSEVIER

Estimating Canopy Water Content of Chaparral Shrubs Using Optical Methods

Susan L. Ustin, Dar A. Roberts,† Jorge Pinzón,* Stephane Jacquemoud,‡ Margaret Gardner,† George Scheer,* Claudia M. Castañeda,* and Alicia Palacios-Orueta**

Predicting fire hazard in fire-prone ecosystems in urbanized landscapes, such as the chaparral systems of California, is critical to risk assessment and mitigation. Understanding the dynamics of fire spread, topography and vegetation condition are necessary to increase the accuracy of fire risk assessment. One vital input to fire models is spatial and temporal estimates of canopy water content. However, timely estimates of such a dynamic ecosystem property cannot be provided for more than periodic point samples using ground based methods. This study examined the potential of three quasiphysical methods for estimating water content using remotely sensed Airborne Visible Infrared Imaging Spectrometer (AVIRIS) data of chaparral systems in the Santa Monica Mountains, California. We examined estimates of water content at the leaf, canopy, and image level and compared them to each other and to ground-based estimates of plant water content. These methods predicted water content (with R^2 *between 0.62 and 0.95) but differ in their ease of use and the need for ancillary data inputs. The prospect for developing regional estimates for canopy water content at high spatial resolution (20 m) from high resolution optical sensors appears promising.* ©*Elsevier Science Inc., 1998*

INTRODUCTION

California's chaparral represents one of several fire-adapted ecosystems and contain many of its rare and endemic species (Minnich, 1983; Mooney, 1988). It is one of the most extensive vegetation types in California, covering 3.5M ha or 5% of the land area of the state (Weislander and Gleason, 1954) and 9% if soft chaparral is included (Holland and Keil, 1990). Chaparral reaches its maximum development in southern California, and these shrublands are typically subject to periodic wildfire at decadal to century frequencies. Fire risk is a major threat in southern California chaparral due to past management, including 60 years of fire suppression (Yool et al., 1985; 1986; Radtke et al., 1982), and because hot, dry late summer winds promote uncontrolled fire (Holland and Keil, 1990). The Mediterranean climate summers coupled with the presence of chaparral communities in the urbanized wildlands of the Santa Monica Mountains make wildfire one of the most serious economic and life-threatening natural disasters faced by the region. Costs of wildfire suppression statewide exceeds $100 million annually with a direct wildfire loss of $65 million (CDF, http://www.fire.ca.gov); many of the largest fires of the past 20 years and the most costly in terms of human and economic loss have been in the Santa Monica Moutain Zone (SMMZ). Furthermore, the steep fire-burned hillsides are also subject to erosion, slumpage, and mud slides during the winter rains that follow late summer wildfires.

The SMMZ is a 630,100 ha east–west trending range with 650 m of vertical relief and located from the center of the greater Los Angeles metropolitan region westward 76 km to the Pacific Coast. More than 60 years of fire suppression (Radtke et al., 1982), and an extensive die back during the 1987–1993 drought, have produced high levels of accumulated fuel in these communities (Ruggelbrugge and Conard, 1996; up to 118 Mg ha^{-1} in our data). A series of fires in the fall of 1993 burned 22,000 ha from Simi Valley in the northeast to the coastal city of Santa Monica within a few hours. Urban encroach-

* Department of Land, Air, and Water Resources, University of California, Davis
† Department of Geography, University of California, Santa Barbara
‡ Laboratoire Environnement et Developpement, Université Paris 7, Paris, France

Address correspondence to Susan L. Ustin, Dept. of Land, Air, and Water Resources, Univ. of California, Davis, CA 95616. E-mail: slustin@ucdavis.edu

Received 13 May 1996; revised 10 December 1997.

REMOTE SENS. ENVIRON. 65:280–291 (1998)

655 Avenue of the Americas, New York, NY 10010

0034-4257/98/$19.00
PII S0034-4257(98)00038-8

ment into the canyons and mountain wildlands have increased fire hazard to critical levels. Developing techniques to monitor fire hazard and predict the spread of fire is of major concern to the region for public safety and to minimize economic loss. One key factor in the susceptibility to fire is the water content of the vegetation canopy. To a first approximation, water content depends on the canopy biomass and the proportion of live canopy-to-litter biomass. However, this assumes that water content of the live canopy remains relatively constant and that variance depends on the hydration state of litter, a function of the relative humidity of the atmosphere. Routine monitoring by Los Angeles Country Fire Department shows that chaparral water content varies significantly by species type at both diurnal and day-to-day scales. The development of imaging spectrometers and new remote sensing techniques provides possible tools to permit monitoring of this dynamic fire risk information.

The purpose of this article was to examine how well variation in canopy water contents can be estimated using optical sensors at the leaf, canopy, and sensor image scales. We obtained reflectance and transmission spectra of leaves in the laboratory and canopy spectra in the field of the dominant chaparral species and estimated water content from the spectra. We chose to compare quasi-physical analytical methods that minimize the need for calibration data to determine water contents. While other methods, such as multiple linear regression or ratio techniques, could be used for estimating water content, they require data-specific calibrations and therefore have shown little potential for more automated applications. Physical models have potential to be extended to image data sets where water content calibration data are not known in advance. In this study, leaf estimates derived from spectroscopy were evaluated by comparison to measured leaf water contents and to other canopy estimates. Water content estimates derived from concurrently acquired Advanced Visible Infrared Imaging Spectrometer (AVIRIS) images 19 October 1994 and 9 May 1995 were evaluated against the leaf and canopy model results and field data.

METHODS AND MATERIALS

Site Selection and Description

At least four distinct chaparral communities exist in a complex spatial mosaic across this range. These species exhibit different sensitivities to fire and responses to post-fire due to growth patterns, density, biomass, and fuel accumulation (Ehleringer and Mooney, 1982; Oechel and Lawrence, 1981; Barrio and Conard, 1991). They exhibit different patterns of water relations (Miller and Poole, 1979; 1980) and ignition/combustion characteristics (Barro and Conard, 1991). The dominant chaparral community in California is known as chamise (*Adenostoma fasciculatum*), which often forms nearly pure stands and is most common on hot south- and west-facing slopes and ridges. *Ceanothus* chaparral is typically midsuccessional and is dominated by one or more species of *Ceanothus* (California lilac). It tends to have lower plant density than chamise but more complete crown cover (Mooney and Miller, 1985; Keeley and Keeley, 1988). Mixed broadleaf Manzanita (*Arctostapylos*) chaparral is generally the most diverse and is often composed of several shrub species and may include grasslands. Mixed chaparral occurs at higher elevations and on deeper soils. Lastly, the coastal region may be dominated by Coastal sage (*Salvia*) species. It is more common at lower elevations below *Ceanothus* chaparral but does occur in isolated patches at higher elevations on outcrops of shallow or fine textured soil (Barbour and Billings, 1988). This latter community tends to maintain the highest foliar density and is greenest to the eye. It tends to be of lower stature (<1.5 m) and lower shrub cover with higher diversity of growth forms than the other communities (Mooney, 1988).

Three sites were selected for detailed canopy reflectance measurements that expressed different community composition types and biomass ranges. Measurement sites expressed little evidence of disturbance and were judged to be representative of their respective chaparral types as selected by professional staff from the National Park Service Santa Monica Research Unit and the USDA Forest Service Fire Laboratory scientists who were familiar with local vegetation patterns. Data from one site, Zuma Ridge are included in this article. It is a low elevation coastal site near the Pacific coast that is composed of areas of young coastal sage and mixed chaparral vegetation. Coastal sage is drought-deciduous and exhibits pronounced seasonal changes in water content. Most species in the community have senescesced by late summer and remain dormant until the following spring. Chamise dominates sites farther inland and undergoes more moderate seasonal senescence. Other sites that were intensively studied were located at Castro Crest (chamise dominated) and Encino Reservoir (inland *Ceanothus* chaparral). Additional plots were selected for estimates of canopy water contents. Locations where samples were measured were recorded by a ProXL (Trimble Navigation, Sunnyvale, CA) Global Positioning System (GPS) having approximately 1 m precision after differential correction. Statistical comparisons were based on regressions between measured and predicted leaf and canopy water contents.

Field Radiometric Data

The ASD full range spectrometer (400–2500 nm; Analytical Spectral Devices, Boulder, CO) with an 18° field-of-view (FOV) was mounted on a bucket truck and above canopy spectra acquired over seven canopies at each site.

Table 1. Site Names, Species Measured, Heights of Detector above Canopy and Corresponding Field of View

	Zuma Site		
Flag	*Dominant Species in FOV*	*Height (m)*	*FOV (m)*
1	*Rhus laurina*	3.4	1.5
2	*Artemisia californica*	3.4	1.5
3	*Salvia leucophylla*	3.0	1.3
4	*Artemisia californica*	3.5	1.5
5	*Artemisia californica*	3.6	1.6
6	*Eriogonum cinereum*	4.5	2.0
7	*Salvia leucophylla*	4.0	1.8

Five replicate spectra (with internal average of 10 spectra) were acquired per canopy (above seven chaparral canopies). The data were noisy in the region of the last spectrometer so wavelengths longer than 1800 nm were not used in the analysis. Locations were identified for repeat measurements: species, canopy height, and spectrometer height were recorded and FOV calculated (Table 1). Canopy spectra were measured six times diurnally at intervals between 0900 h and 1700 h Pacific Standard Time to examine any sun-view angle reflectance changes and monitor for possible diurnal changes in canopy water content. A Spectralon panel (Labsphere, Inc., North Sutton, NH) was mounted on a tripod attached to the bucket and adjusted normal to the ground using a leveling device for corrections to apparent surface reflectance. Corrections for Spectralon were postprocessed to produce absolute 100% reflectance.

Field Vegetation Data

The Forest Service Fire Laboratory and the Los Angeles County Fire District harvested above ground canopy biomass from eight 5 m×5 m plots. Total plot biomass was weighed in the field. A subsample of the biomass was measured for water content, leaf mass, and live and standing litter stem mass, and number of shrubs ha^{-1} for the June data acquisition. GPS locations were obtained at site corners. Percent canopy moisture (water weight/dry weight) by species was measured by the Forest Service at 13 additional sites; some plants were harvested in June and October. Sixteen additional polygons of seven vegetation types were measured for comparison to AVIRIS data (587 pixels) by Gardner (1997) and Roberts et al. (1998, this issue).

Leaf and Canopy Biophysical Measurements

Water content was estimated for the canopy within the FOV of the ASD at the time of canopy spectral measurements. Five foliar samples were collected for each species by cutting a branch (at least 10 leaves, including flowers where present). Selected samples that were located near the spectral measurements and attempts were made to collect branches representative of the condition of the sample in the FOV. Water content measurements were made coincident with spectral measurements through the day. For large leaves, the fresh weight of 3.46 cm^2 disks were cut using a cork borer and immediately weighed using a portable electronic balance, Model XD1200D balance (Denver Instrument Co., Denver, CO). For small leaves, we weighted entire blades and measured the area using a Canon Video Visualizer RE-650 camera and a digitizer. After weighing, samples were placed in paper bags and dried at 70°C for 4 days or until dry weights were constant. Stems, remaining leaves, and flowers of branch samples were measured for fresh weight (FW) and dried to obtain leaf and stem fresh weight and dry weight (DW).

Laboratory Radiometric Data

For most species, both leaf reflectance and transmittance were measured in the lab on a CARY 5E spectrophotometer (Varian, Inc. Sunnyvale, CA), in a 150-m integrating sphere model RSA-CA-50D (Labsphere, Inc. North Sutton, NH) with a Spectralon surface. We acquired reflectance spectra for all species at the site, over the spectral region between 400 nm and 2500 nm with an interval of 2 nm; for *Adenostoma fasiculatum* (chamise) and *Artemisia californica* (sagebrush) which have needle-like leaves (see Table 1), the transmittance could not be measured so that only the infinite reflectance of an optically thick sample was obtained.

Advanced Visible Infrared Imaging Spectrometer Data (AVIRIS) Data

Advanced Visible Infrared Imaging Spectrometer Data (AVIRIS) were acquired over the Santa Monica Mountains on 19 October and 9 May 1995 and corrected to apparent surface reflectance using a modified version of the Modtran III radiative transfer atmospheric code using the algorithm developed by Green et al. (1995; 1996) and Roberts et al. (1993). This model accounts for a spatially variable atmosphere, such as found over mountainous terrain. It was used to calculate apparent surface reflectance in the 1995 AVIRIS images (Green et al., 1995; 1996; Roberts et al., 1998, this issue). A best-fit estimate of the equivalent water vapor and liquid water thicknesses are generated for each pixel by fitting across 20 bands centered on the 940 nm atmospheric water vapor band (Roberts et al., 1998b). A high spectral resolution imaging sensor like AVIRIS can separate the water vapor in the atmospheric column from the liquid water content of the surface due to the 20 nm wavelength separation between peak absorptions of water in vapor and liquid forms (Green et al., 1995; 1996; Roberts et al., 1993). These two new data products, uniquely available from AVIRIS images, have not ben explored for their potential to contribute to surface water content information. The scenes were georeferenced to a SPOT image with an overall spatial accuracy of ~10 m. Data shown are sub-

sets of merged flight lines that cover a 13×17 km area extending between the city of Thousand Oaks in the interior to the city of Malabu at Point Dume on the coast.

Reference endmembers were selected from spring and fall spectral libraries of soils, leaves, canopies and NPV developed for the Santa Monica Mountains (Gardner, 1997; Roberts et al., 1998). Standard mixture analysis followed the methods of Smith et al. (1990), but these were modified in the following way: Most of the image could be described by three or four endmember models, but these are found in different areas of the image. We show results from merging the following three endmember models (soil+NPV+shade, GV+NPV+shade, and GV+soil+shade). Previous results reported by Roberts et al. (1993) found that the dimensionality of AVIRIS was typically low and solving for more endmembers resulted in an unstable solution. In this case, we select the optimal set for each pixel based on a best fit RMS criterion (Painter et al., 1998, this issue).

Data Analysis

Two quasiphysical analytical methods were investigated for estimating leaf and canopy water content in the chaparral species. The first method applied a modified version of the PROSPECT model (Jacquemoud et al., 1996), which predicts several canopy chemistry variables including water thickness from reflectance data. PROSPECT is a radiative transfer model which describes a leaf as a simple plate composed of photosynthetic pigments, water, and cell wall matrix (Jacquemoud and Baret, 1990). The modified model predicts leaf optical properties using specific absorption coefficients for pigments, nitrogen, carbon, cellulose, lignin, and water which were developed and tested from the LOPEX93 experiment leaf chemistry data set (Hosgood et al., 1995; Jacquemoud et al., 1995; ACCP, 1994). The model using the LOPEX93 absorption coefficients, including a calculated cell water coefficient, was run in the foreword direction on laboratory measured leaf spectra from species collected in the Santa Monica Mountains and the best fit reflectance and transmission were iteratively fit to the measured reflectance and transmission spectra. The full spectrum from 400 nm to 2500 nm was used because previous results of Jacquemoud et al. (1996) have shown that the optical region contributes to the better estimation of leaf water than using the infrared alone. The inversion model estimates leaf biophysical properties and in this case, we report only estimates for water content, estimated as mg H_2O g^{-1} dry weight or mg H_2O cm^{-2}. Forty leaf reflectance and transmittance samples were iteratively fitted and water content determined using the modified PROSPECT model. Because this model has been tested on a wider range of data sets, these results were used to compare and validate the next analytical method, which was applied at leaf, canopy, and image scales.

The second analytical method used a new technique that extends the foreground/background method of Smith et al. (1994) using techniques described by Pinzon et al. (1998) termed Hierarchical Foreground/Background Analysis (HFBA). HFBA divides spectral measurements into foreground and background spectral groups based on the properties of the selected training spectra. This is accomplished by sequentially deriving a series of weighing vectors that extract features at different levels of detection. In this case it corresponds to variation in the water content of the canopies and defines the ranges of variation. The first step of the HFBA normalizes each spectrum to reduce dependency on the measurement conditions. The HFBA vector is constructed using a few training samples that carry the spectral information about water content. The HFBA methodology is based on the concept that the leaves and canopies are biochemical mixtures that are not simple linear operators but where nonlinearities can be reduced by sequential discrimination at different concentration ranges. This reduces the range of variance at each step and may account piecewise for the effects of nonlinearities. The singular value decomposition (SDV) procedure efficiently focuses the spectral information to fit the chemistry over a specified range. The energy packing that results from SDV defines the detectable level of variation at each subsequent level. Discrimination is bounded by instrument uncertainty, nonlinear spectral dependencies on geometry and composition, and on the condition under which the experiment was performed. The full leaf spectrum was used to estimate leaf water concentrations for consistency with the PROSPECT results. Grossman et al. (1994) showed that plant pigment concentrations were highly correlated with leaf water content in their study. While we ran comparison vectors using only the infrared part of the spectrum, best results were obtained when both visible and infrared spectral regions were included. For the canopy measurements, we did not use the wavelengths longer than 1800 nm and recalculated the HFBA vectors from the leaf measurements for this spectral region. These data were omitted from the analysis because of noise problems. HFBA calculated for the AVIRIS images for October 1994 and May 1995 used the full spectrum minus several bands having a high noise content.

Chaparral species tend to have low water contents (ranging between 55% and 65% in our samples) as all exhibit some degree of sclerophylly. Mean specific leaf weights for common species are shown in Table 2. Although the stratification effectively discriminates samples into different ranges of water content, it is based on spectral differences and therefore does not require any predetermined knowledge of the actual water content to run the analysis. Pinzón et al. (1998) describes rules for semiautomated application of this classification. Once the vectors are obtained, they can be applied to unknown samples. In this case we used 11 spectra to train the leaf

Table 2. Mean Specific Leaf Weight (SLW) of the Dominant Species at the SMM Sites, Measured in June 1995

Species	*Mean SLW (mg cm^{-2})*
Arctostaphylos glandulosa	33.005
Rhus laurina	14.458
Eriogonum cinereum	10.018
Ceanothus oliganthus	12.227
Haplopappus sp.	11.305
Ceanothus spinosus	12.664
Quercus dumosa	16.701
Artemisia californica	14.746
Adenostoma fasiculatum	15.856
Salvia sp.	11.789

vectors and applied it to 62 leaf spectra. Leaf water vectors were applied to the AVIRIS spectra and modified vectors that used only the 400–1800 nm wavelength range were applied to the canopy spectra. AVIRIS-derived water contents were compared to field measurements and to the water contents derived from the atmospheric correction.

RESULTS

Leaf and Canopy Spectra

Figure 1a shows an example of leaf reflectance and transmission of an evergreen schlerophyllic species typical of chaparral vegetation. Figure 1b provides several examples of the variation in leaf reflectance among species and one example of floral reflectance. Considerable differences in spectral characteristics are evident; especially in the 600–700 nm region, the 970 nm and 1200 nm water band depths, and other differences in the SWIR region. Diurnal spectral measurements showed only minor variation due to changes in solar zenith nor did leaf water content measurements reveal substantial diurnal changes in water content between 1000 h and 1700 h. Our measurements indicate less then 5% diurnal variance in water concentration (g g^{-1}) within individual plants while differences in water contents between species were large (Table 2). Therefore, the diurnal spectral data were averaged by plot and not considered separately. Near-infrared reflectance at the canopy scale was generally lower than the comparable leaf spectra and spectra were somewhat more noisy. Leaf and canopy water absorptions at 970 nm and 1200 nm are evident as is atmospheric water absorption at 1470 nm; the 970 nm absorption was noisy due to poor sensitivity of the ASD in the 900–1000 nm spectral region.

PROSPECT Leaf Optical Properties Model

The PROSPECT model predictions for foliar water thickness of leaf spectra are shown in Figure 2a. We used two models having different water absorption coefficients, one was based on the Curcio and Petty (1951) theoretical estimate for pure water and the other was the derived absorption coefficient from the LOPEX93 experiment (Jacquemoud et al., 1996). The predicted water thickness was always higher when the theoretical water absorption coefficient was used. Both models overestimated the measured leaf water thickness, although the LOPEX93 model produced a closer approximation of leaf water thickness (Fig. 2b). This model accurately predicted leaf water thickness (r^2=0.95) in the LOPEX study for a data set of leaves having a greater range of water contents (Jacquemoud et al., 1996). The regression prediction for these samples is r^2=0.73. The relative error was greatest for the highest water content leaves.

Figure 1. Leaf optical properties of the few samples collected in the Zuma site: a) reflectance and transmittance spectra of Laurel Sumac (*Rhus laurina*); b) reflectance spectra of *Eriogonum cinereum* leaf (e), *Salvia leucophylla* leaf (s) and flower (s_f), *Rhus laurina* leaf (m), and *Artemisia californica* leaf (a).

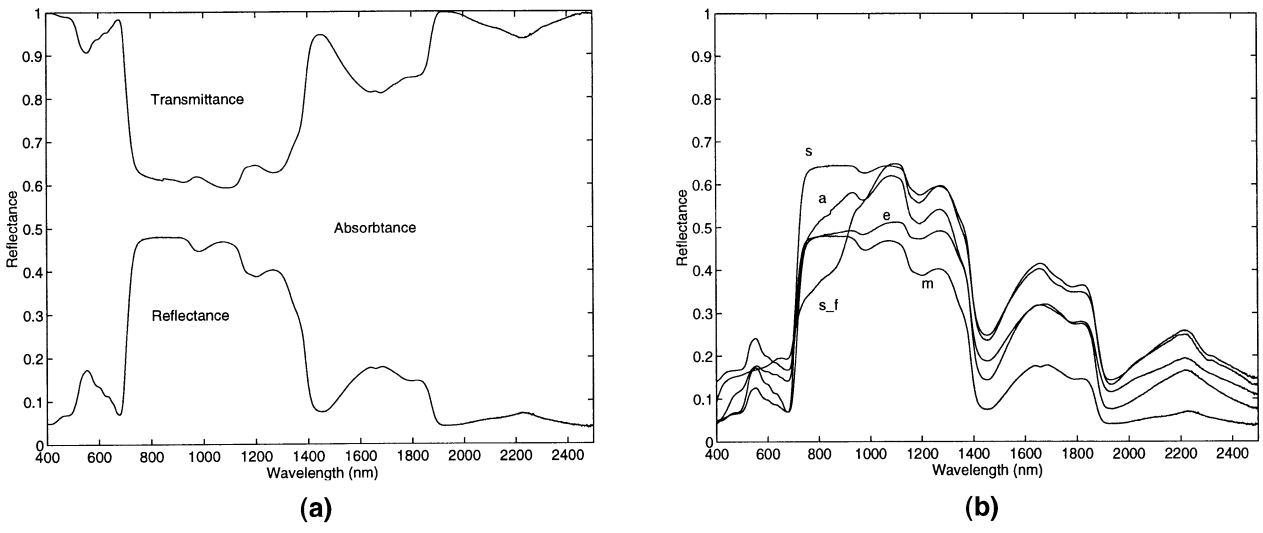

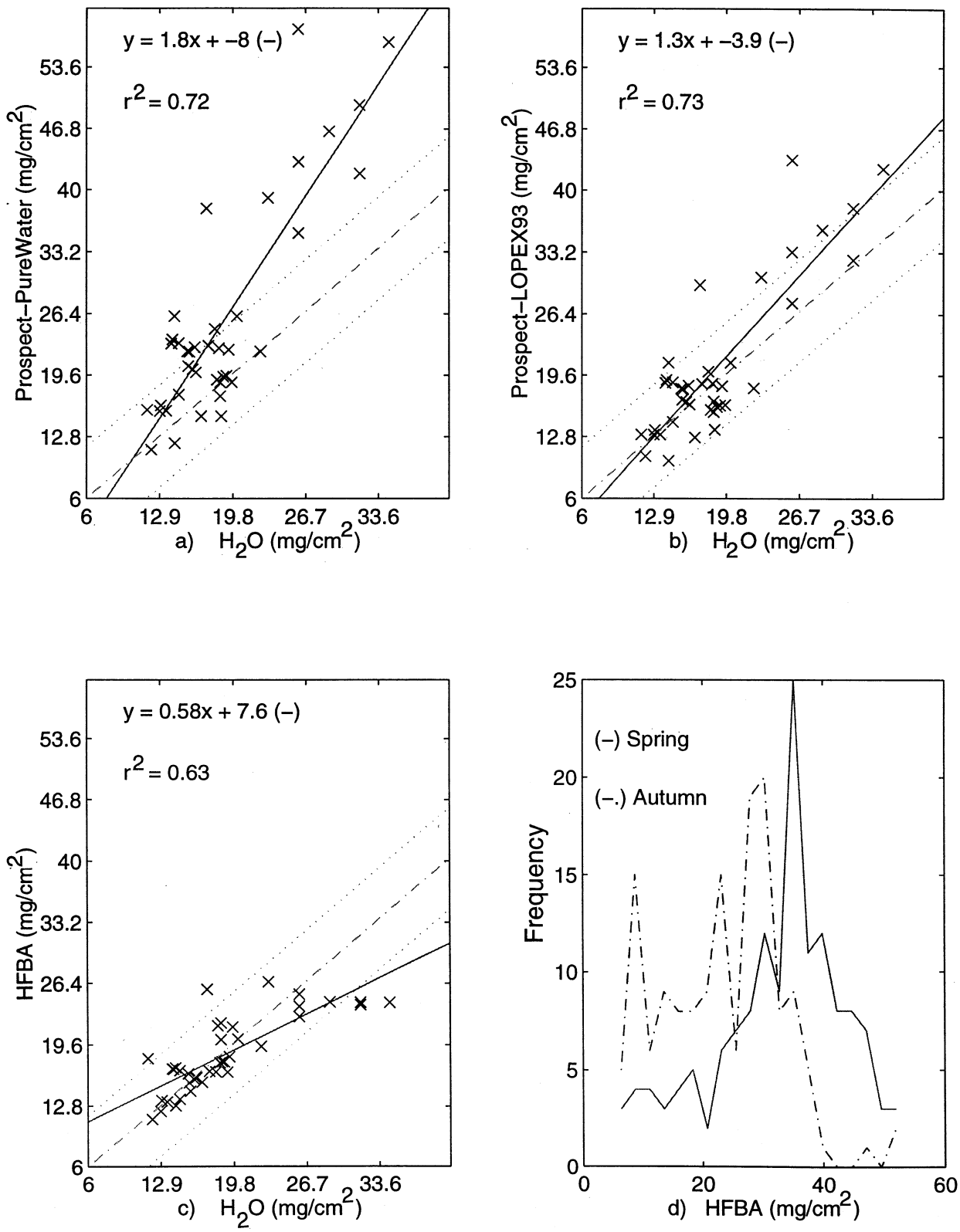

Figure 2. a) PROSPECT model predictions for foliar water thickness of Santa Monica leaf spectra for the absorption coefficient of pure water based on Curcio and Petty (1951). b) Absorption coefficient for *in situ* water derived from the LOPEX93 experiment (Jacquemoud et al., 1996). c) Prediction of leaf water using the HFBA method. The reflectance and water data set is the same as in a) and b). d) This panel shows the histogram of the water concentrations derived from the HFBA vector applied to the Zuma site canopy data for spring and autumn.

To use the PROSPECT model at the canopy or image scale requires linking it to a canopy reflectance model. Although the PROSPECT model has been linked to SAIL, a simple canopy model (Jacquemoud, 1993), and to more physically realistic canopy models, it requires additional data about canopy structure and its spatial distribution. At this time we lack sufficiently detailed canopy structural data to evaluate the model predictions and so they were not included here. However, because the PROSPECT model is widely accepted, the accuracy of the model's prediction of water content provides a basis to compare the reliability of the other models we consider.

HFBA Model

Leaf Reflectance

Initially we applied HFBA to the leaf reflectance data set from SMMZ using a water vector adopted to low water content sclerophytic species to determine the relative prediction of water content (Fig. 2c). Initially, we used a "standard" water vector that was derived from a subset of the LOPEX93 data set (Pinzón et al., 1995; 1998). However, it gave low predictions because it was not sufficiently sensitive to the low values of water content of SMM samples. The overestimated water content produced a pattern similar to that found for the "pure" water absorption coefficient used in PROSPECT. By selecting a training set of 11 spectra that spanned the range of water contents found in the SMM, the scaling effect was fixed, and we retained better predictions for both the training and validation data sets. In this case, only two samples of 40 had predicted water contents that were outside an acceptable estimate. Figure 2c shows the regression relationship between predicted and measured water content for the general water vector which has an r^2=0.62 and a slope near 1. Thus, the predictions of leaf water content are of comparable accuracy to those derived from the PROSPECT model but require less information to predict the water concentration.

Canopy Reflectance

The water content of the canopy samples were overestimated when the leaf vector was applied because of the strong absorption in the leaf data sets around 1800 nm. Eliminating the bands between 1300 nm and 1478 nm and wavelengths longer than 1800 nm and recalculating the vector caused an insignificant shift in leaf predictions and a better fit to the canopy data, despite potential problems scaling between leaves and canopies. Therefore, the modified leaf vector was used to analyze for canopy water contents. Figure 2d shows the histogram distributions for the prediction of water content in the spring and autumn. The normalized error is about 0.4 (standard deviation); only two samples exceed 1 standard deviation. The HFBA predication clearly shows greater water contents in spring (3.3 g dm^{-2}) than autumn (mean=2.8 g dm^{-2}). These changes are realistic for seasonal changes in canopy water content and are within the ranges of SLW shown in Table 2.

AVIRIS Water Content

A three-band pseudocolor image of the Point Dume area (Pacific coast) is shown for October 1994 and May 1995 (Fig. 3). The most striking difference between the images is the apparent seasonal increase in the abundance of green vegetation in the spring (as indicated by the increase in near-infrared reflectance, shown by the 838 nm band). The October image was acquired near the end of the summer drought while the May image was obtained near peak seasonal greenness. The surf/shoreline is observed at the coastal margin, and the city of Malibu is seen on Point Dume. The distribution of chaparral is primarily located in the mountains to the north of the shoreline. Irrigated golf courses stand out from the native vegetation as light green patches, which can be found near the midleft and lower right margins of the images. A network of roads crossing the mountains is also apparent. Three small reservoirs are seen in the northwest corner and two smaller ones are found nearer the center of the image.

A comparison of the spectral mixture analysis fractions from green vegetation, soil, and nonphotosynthetic (litter) endmembers is shown in Figure 3. Few pixels have pure bare soil exposures (seen as blue) in either autumn or summer. The relative fractions of soil and litter are high in the autumn while the May image shows the fractions of green vegetation and soil are highest (Fig. 3d). The golf courses stand out in both seasons because of irrigation. The coastal sage chaparral community is autumn deciduous and is distinguished in the images as red or orange patches near the coast in the October data (Fig. 3c).

The atmospheric water vapor images and liquid water thicknesses for the two scenes are shown in Figure 4. Significant seasonal differences in liquid water thickness and concentration are apparent between the autumn and early summer dates (Figs. 4b,c,e,f). While validation data are limited, the Point Dume scene shows reasonable spatial patterns with higher water vapor density along the coast and in the valleys and least near the ridges. The patterns seen in the water vapor images closely match the topography when compared to a digital elevation model. The water vapor concentration above the ocean and lakes shows an apparently high water vapor density (near 24 mm and displayed as white); however, this is an artifact due to the low radiance reflected from water surfaces.

The liquid water maps derived from the atmospheric correction (Figs. 4b,e) and HFBA produce similar patterns (Figs. 4c,f). To evaluate these results, we compared them to other image-derived estimates and to each other by regression analysis. Figures 5a,d show the relations

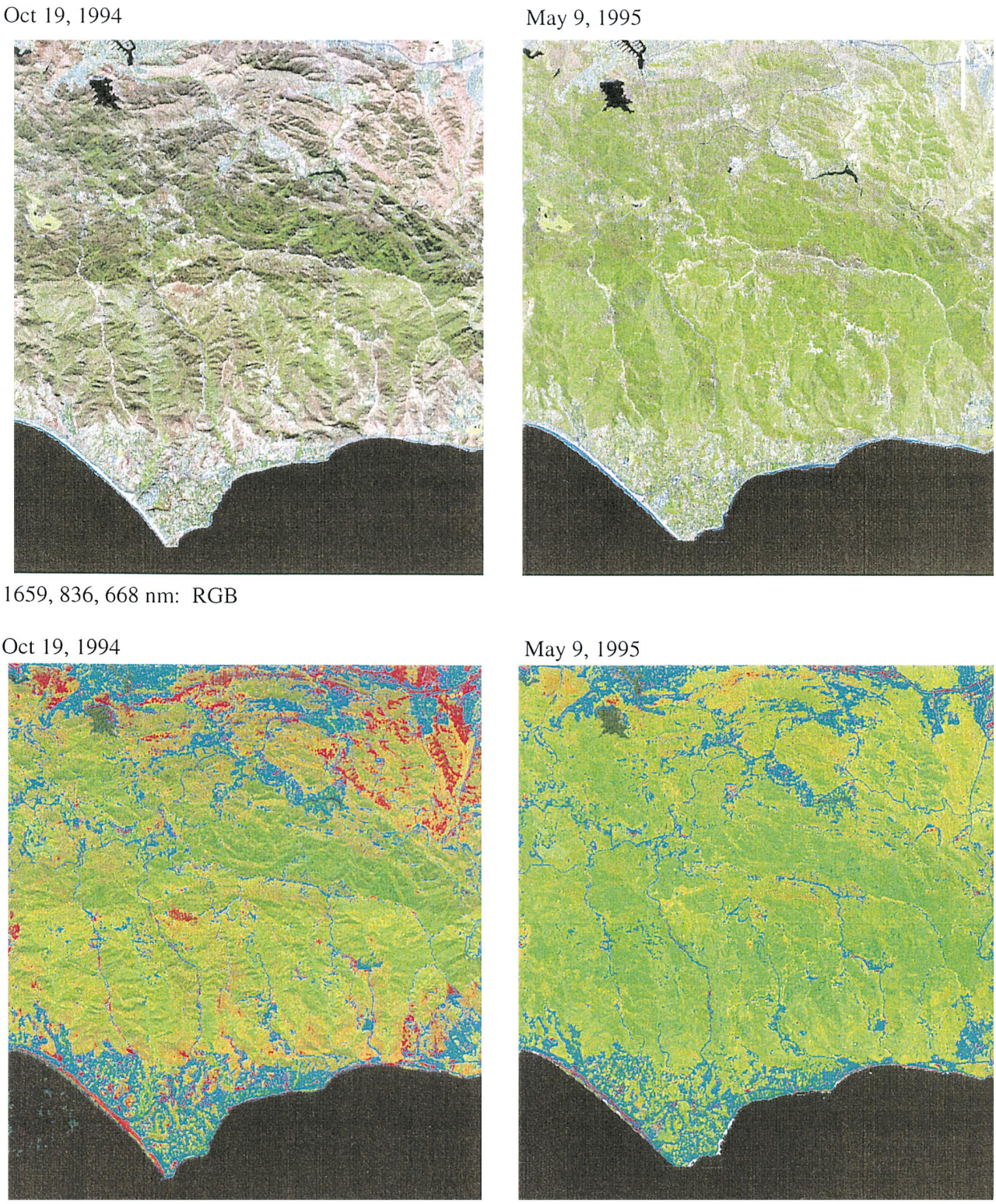

Figure 3. A three-band pseudocolor image from AVIRIS data of the Point Dume area is shown a) for October 1994 and b) May 1995. A false color composite of the spectral mixture analysis fractions for green vegetation (shown as green), soil (red), and nonphotosynthetic stems and litter (blue) endmembers is shown for c) October 1994 and d) May 1995.

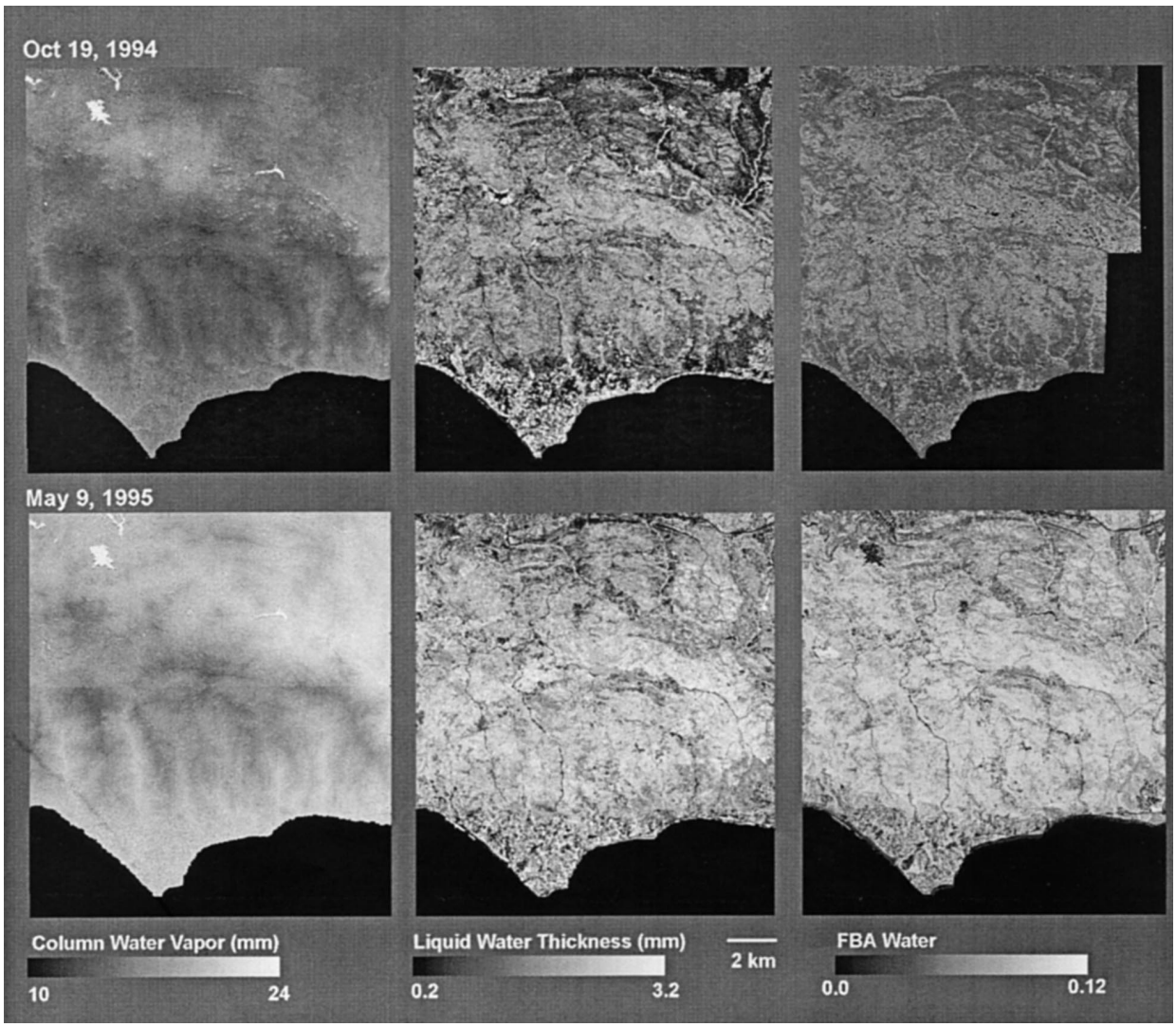

Figure 4. a) The water vapor images derived from atmospheric correction of AVIRIS for October 1994. b) Liquid water thickness derived from the atmospheric correction for October 1994. c) Prediction of liquid water concentration based on HFBA and AVIRIS for October 1994. d) Water vapor images derived from atmospheric correction of AVIRIS for May 1995. e) Liquid water thickness derived from the atmospheric correction for May 1995. f) Prediction of liquid water concentration based on HFBA of AVIRIS for May 1995.

between the atmospheric correction prediction of liquid water thickness and nonphotosynthetic vegetation (NPV) for October 1994 and May 1995. Figures 5b,e show green vegetation (GV) fraction (from the SMA results) compared to the liquid water thickness for October 1994 and May 1995. Figures 5c,f show the HFBA results compared to the liquid water thickness estimates for October 1994 and May 1995. Data are based on 587 pixels representing 16 polygons distributed among seven different chaparral and riparian woodland vegetation types. Vegetation types were mapped by Gardner (1997) in the Point Dume area using techniques described in Roberts et al. (1998; 1997). Liquid water thickness was significantly negatively correlated with NPV and positively correlated with GV. The slope and intercept of the relationship changes between the dates as does the scatter around the regression line, which was opposite between GV and NPV. At low NPV the relationship to water content is less, possibly because of misclassification of NPV with soil. In contrast, the relationship between water content and GV is more noisy at high water concentrations in the autumn and has a wider range (and lower correlation) in the spring. This may indicate that the relationship becomes less predictive at high GV fractions but is accurate over the low values of concern for fire risk assessment. There is a significant positive correlation between the liquid water thickness derived from the atmospheric correction and the HFBA also, although not as tightly coupled as the former is to the vegetation fractions. In this case, the slope and intercept of the relationship between

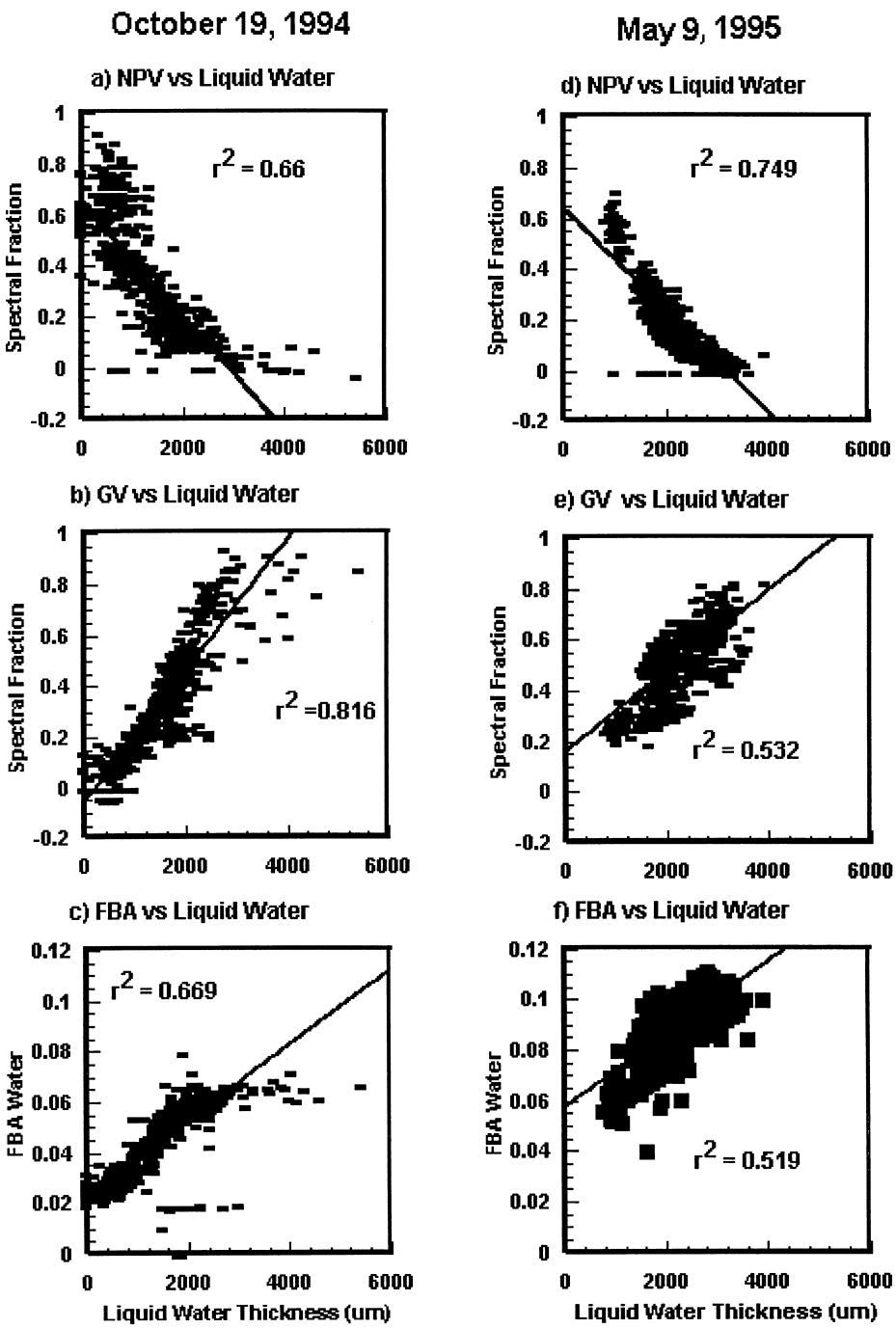

Figure 5. This figure shows the correlation a) the NPV fractions from AVIRIS vs. atmospheric correction derived liquid water thickness for October 1994 and d) the NPV fractions from AVIRIS vs. atmospheric correction derived liquid water thickness for May, 1995. b) The GV fractions vs. atmospheric correction derived liquid water thickness for October 1994, e) the GV fractions vs. atmospheric correction derived liquid water thickness for May 1995. c) The HFBA-derived water concentrations from AVIRIS for October 1994, and f) the HFBA-derived water concentrations from AVIRIS for May 1995.

the liquid water thickness and the HFBA water remained constant between autumn and spring AVIRIS images, but the distribution was somewhat changed. In the autumn both high and low values of HFBA predictions differ from estimates of liquid water thickness, but intermediate values are close. Both methods predict higher water contents in the May data and show a similar range of variance. At this time the differences in variance between these variables cannot be evaluated; however, they provide a basis for developing hypotheses about the conditions under which these relationships are predicted to be close and where they should become more independent.

DISCUSSION

Spectral detection and quantification of leaf and canopy water content seems possible from airborne or space-

borne imagery. We used several quasiphysical spectral analysis methods to examine remote measurement of water content of chaparral species at leaf, canopy, and image scales. The methods differ in their expectations for input information and their ease of use in application but also in their robustness and accuracy of prediction. Our results show significant seasonal and spatial changes in water content at all scales between leaf, canopy and images. While these are largely observations of phenological processes, they illustrate the dynamic and spatially complex variation in canopy water concentration. The correlations but not equivalence between water concentration and canopy greenness support the contention that these variables are not entirely correlated and that a map of canopy greenness is not identical (e.g., compare Figs. 3 and 4).

The retrieval of equivalent liquid water thickness from a modified MODTRAN II radiative transfer atmospheric code was derived by fitting the reflectance across a water absorption feature at 940 nm and comparison to the absorption that is caused by different water thickness. The other methods we examined utilized the full reflectance spectrum, and included the PROSPECT leaf optical properties model (Jacquemoud et al., 1996), and a spectral decomposition method for water retrieval, termed Hierarchical Foreground/Background Analysis (Pinzón et al., 1998). At the leaf scale both PROSPECT and HFBA give similar accuracies of prediction of water concentration ($r^2 \approx 0.7$). In both cases, we are beginning to understand how the natural variation in leaf water content or concentration affects reflectance and how to scale the properties to obtain reasonable estimates. While bias in the choice of calibration spectra used in statistical models has long been recognized as causing difficulty in extending remote sensing results beyond the calibration site; however, we have lacked a systematic means for determining which characteristics should be included and which excluded to obtain a stable prediction. The hierarchical method combined with noise analysis provides a means to make this determination. Accurate representation of an unknown population requires an estimate of the mean properties and the weighted variance. The HFBA method showed that it is possible to scale predictions between the leaf and canopy measurements despite uncertainties and obtain frequency distributions consistent with measurements of typical shrub canopies and water concentrations. This scaling is partially due to the low leaf area indices of these species at the measurement sites, which were approximately 1. The estimated liquid water content or concentration of the canopy is somewhat less accurately predicted, but this error is partially attributed to canopy measurement errors. Because the fractions are used to evaluate the water predictions, it is necessary to understand the factors affecting these estimates. One physical reason for variance in the endmember fractions is that shade can vary independently of the fractional cover of a site or amount of NPV. Therefore, variation in shade content will modify the NPV fraction even when no liquid water is present. A second reason is that the soil surface in these semiarid sites was dry in May and October when the AVIRIS was acquired. Because the soil and NPV have an insignificant concentration of liquid water, how they interact may bias or diminish the relationship to canopy water concentration. As a result, in areas of sparse or senescent vegetation we see the relationship between NPV and liquid water break down because the pixel also has exposed soil in it.

We wish to thank Dr. Ray Sauvijot of the National Park Service for the Santa Monica Mountains and Dr. Susan G. Conard and Mr. John Rugglesbrugge, U.S. Forest Service Fire Laboratory, and Mr. Jimmie L. Pyland, Deputy Fire Chief, Los Angeles Fire District, for their assistance in supporting this study. We wish to thank Martha Diaz Barrios for field support and help with the graphics. This research was funded by a grant from NASA Terrestrial Ecosystems and Biogeochemical Dynamics Branch, NAGW-4626-I. We wish to thank the Digital Equipment Corporation for providing the DEC Alpha computers under the Sequoia 2000 Grant Cooperative Research Agreement #1243.

REFERENCES

ACCP (1994), NASA Accelerated Canopy Chemistry Program, Final Report NASA-EOS-IWG, NASA, Greenbelt, MD, 19 October.

Barbour, M. G., and Billings, D. W., Eds. (1988), *North American Terrestrial Vegetation,* Cambridge University Press, New York, 434 pp.

Barro, S. C., and Conard, S. G. (1991), Fire effects on California chaparral systems—an overview. *Environ. Int.* 17: 135–149.

Curcio, J. A., and Petty, C. C. (1951), The near infrared absorption spectrum of liquid water. *J. Opt. Soc. Am* 41: 302–304.

Ehleringer, J., and Mooney, H. A. (1982), Productivity of desert and mediterranean-climate plants. In *Physiological Plant Ecology, IV* (O. L. Lange, P. S. Nobel C. B. Osmond, and H. Ziegler, Eds.), Springer-Verlag, New York, pp. 205–231.

Gardner, M. (1997), Mapping chaparral with AVIRIS using advanced remote sensing techniques, Ph.D. dissertation, Department of Geography, University of California, Santa Barbara, 58 pp.

Green, R. O., Conel, J. E., and Roberts, D. A. (1995), Measurement of atmospheric water vapor, leaf liquid water and reflectance with AVIRIS in the Boreal–Ecosystem–Atmosphere Study: initial results. In *AVIRIS Imagery, Summaries of the 5th Annual Jet Propulsion Laboratory's Airborne Earth Science Workshop* (R. O. Green, Ed.), JPL 95-1, Jet Propulsion Laboratory, Pasadena, CA, Vol. 1, pp. 95–98.

Green, R. O., Roberts, D. A., and Conel, J. E. (1996), Characterization of the atmosphere and inversion of AVIRIS calibrated radiance to apparent surface reflectance. In *Summaries of the 6th Annual Jet Propulsion Laboratory's Airborne Earth Science Workshop* (R. O. Green, Ed), JPL 96-4, Jet Propulsion Laboratory, Pasadena, CA, Vol. 1: pp 135–146.

Grossman, Y. L., Sanderson, E., and Ustin, S. L. (1994), Rela-

tionships between canopy chemistry and reflectance for plant species from Jasper Ridge, California. In *Proceedings International Geoscience and Remote Sensing Symposium IGARSS '94,* 8–12 August, California Institute of Technology, Pasadena, CA.

Holland, V. L., and Keil, D. J. (1990), *California Vegetation*, 4th ed., Biological Sciences Department, California Polytechnic State University, San Luis Obispo.

Hosgood, B., Jacquemoud, S., Andreoli, G., Verdebout, J., Pedrini, G., and Schmuck, G. (1995), Leaf Optical Properties Experiment 93 (LOPEX93), Report EUR-16095-EN, European Commission, Joint Research Centre, Institute for Remote Sensing Applications, Ispra, Italy.

Jacquemoud, S. (1993), Inversion of the PROSPECT+SAIL canopy reflectance model from AVIRIS equivalent spectra: theoretical study. *Remote Sens. Environ.* 54:1281–292.

Jacquemoud, S., and Baret, F. (1990), PROSPECT: a model of leaf optical properties spectra. *Remote Sens. Environ.* 34: 75–91.

Jacquemoud, S., Verdebout, J., Schmuck, G., Andreoli, G. and Hosgood, B. (1995), Investigation of leaf biochemistry by statistics. *Remote Sens. Environ.* 54:180–188.

Jacquemoud, S., Ustin, S. L., Verdebout J., Schmuck, G., Andreoli, G., and Hosgood, B. (1996), Estimating leaf biochemistry using the PROSPECT leaf optical properties model. *Remote Sens. Environ.* 56:194–202.

Keeley, J. E., and Keeley, S. C. (1988), Chaparral. In *North American Terrestrial Vegetation* (M. G. Barbour and D. W. Billings, Eds.), Cambridge University Press, New York, pp. 165–207.

Miller, P. C., and Poole, D. K. (1979), Patterns of water use by shrubs in southern California. *For. Sci.* 25:84–97.

Miller, P. C., and Poole, D. K. (1980), Partitioning of solar and net irradiance in mixed chamise chaparral in southern California. *Oecologia* 47:328–332.

Minnich, R. A., (1983), Fire mosaics in southern California and northern Baja California. *Science* 219:1287–1294.

Mooney, H. A. (1988), Southern coastal scrub. In *Terrestrial Vegetation of California* (M. G. Barbour and J. Major, Eds.), California Native Plant Soc. Special Publ. 9, Sacramento, CA, pp. 471–490.

Mooney, H. A., and Miller, P. C. (1985), Chaparral. In *Physiological Ecology of North American Plant Communities* (B. F. Chabot and H. A. Mooney, Eds.), Chapman and Hall, New York, pp. 213–231.

Oechel, W., and Lawrence, W. (1981), A comparison of vegetation function in two Mediterranean type ecosystems. In *Carbon Allocation and Utilization in Resource Use by Chaparral and Matorral* (P. C. Miller, Ed.), Springer-Verlag, New York, pp. 185–235.

Painter, T. H., Roberts, D. A., Green, R. O., and Dozier, J. (1998), Improving mixture analysis estimates of snow-covered area from AVIRIS data. *Remote Sens. Environ.* 65:320–332.

Pinzón, J. E., Ustin, S. L., Hart, Q. J., Jacquemoud, S., and Smith, M. O. (1995), Using foreground/background analysis to determine leaf and canopy chemistry. In *AVIRIS Imagery, Summaries of the 5th Annual JPL Airborne Earth Science Workshop* (R. O. Green, Ed.), JPL 95-1, Pasadena, CA, pp. 129–132.

Pinzón, J. E., Ustin, S. L., Castenada, C., and Smith, M. O. (1998), Investigation of leaf biochemistry by foreground/background anlaysis, *IEEE Trans. Geosci. Remote Sens.,* in press.

Radtke, K. W. -H., Arndt, A. M., and Wakimoto, R. H. (1982), Fire history of the Santa Monica Mountains. In *Proc. Symp. Dynamics and Management of Mediterranean-Type Ecosystems,* San Diego, CA, USFS Gen Tech. Rep. PSW-58, pp. 438–443.

Roberts, D. A., Adams, J. B., and Smith, M. O. (1993), Discriminating green vegetation, non-photosynthetic vegetation and soils in AVIRIS data. *Remote Sens. Environ.* 44(2/3): 255–270.

Roberts, D. A., Gardner, M., Church, R., Ustin, S. L., and Green, R. O. (1997), Optimum strategies for mapping vegetation using multiple endmember spectral mixture models. In *Imaging Spectrometry III, 42nd Annual SPIE Meeting,* SPIE Conf. Vol. 3118, 27 July–1 August, San Diego, CA, pp. 108–119.

Roberts, D. A., Gardner, M., Church, R., Ustin, S. L., Scheer, G., and Green, R. O. (1998), Mapping chaparral in the Santa Monica Mountains using multiple endmember spectral mixture models, *Remote Sens. Environ.* 65:267–279.

Roberts, D. A., Green, R. O., and Adams, J. B. (1997), Temporal and spatial patterns in vegetation and atmospheric properties from AVIRIS, *Remote Sens. Environ.* 62(3): 223–240.

Ruggelbrugge, J. C., and Conard, S. G. (1996), Biomass and fuel characteristics of chaparral in southern California. In *13th Conf. Fire and Forest Meteorology,* 27–31 October, Lorne, Australia.

Sanderson, E. W., Zhang, M., Ustin, S. L., and Rejmankova, E. (1998), Geostatistical scaling of canopy water content in a California salt Marsh, *Landscape Ecol.* 13:79–92.

Smith, M. O., Ustin, S. L., Adams, J. B., and Gillespie, A. R. (1990), Vegetation in deserts I. A regional measure of abundances from multispectral images. *Remote Sens. Environ.* 29:1–26.

Smith, M., Roberts, D., Hill, J., et al. (1994), A new approach to quantifying abundances of materials in multispectral images. In *Proc. Int. Geosci. and Remote Sens. Symp. (IGARSS '94),* Pasadena, CA, 8–12 August.

Wieslander, A. E., and Gleason, C. H. (1954), Major brushland areas of the coast ranges and Sierra-Cascade foothills of California, USDA For. Ser. PSW For. & Range Exp. Sta. Misc. Pap. PSW-15, U. S. Department of Agriculture, Washington, DC, 8 pp.

Yool, S. R., Eckhardt, D. W., and Consentino, M. J. (1985), Describing the brushfire hazard in southern California. *Anal. Assoc. Am. Geograph.* 75:431–442.